An analog of double electromagnetically induced transparency with extremely high group indexes

An Yang (杨 安)[1], Changchun Yan (闫长春)[1*], Jiebing Tian (田洁冰)[1], Cheng Wang (王 成)[1], Guiming Li (李贵明)[1], and Daohua Zhang (张道华)[2]

[1]*School of Physics and Electronic Engineering, Jiangsu Normal University, Xuzhou 221116, China*

[2]*School of Electrical and Electronic Engineering, Nanyang Technological University, 639798, Singapore*

[*]*Corresponding author: yancc@jsnu.edu.cn*

Received December 25, 2012; accepted January 27, 2013; posted online April 19, 2013

An asymmetric metamaterial exhibiting an analog of double electromagnetically induced transparency (EIT) in the middle-infrared region is reported. The metamaterial consists of two-layered arrays of U-shaped rings embedded in a medium, with the lower layer rotated by 90°. Our simulations demonstrate that both maximum group indexes are extremely high at the two EIT-like positions. The group index reaches about thrice the currently reported maximum value at the high-frequency EIT-like position. The transmittance at the two transparency positions also possesses extremely high Q factors, which is conducive to controlling the propagation of electromagnetic waves.

OCIS codes: 160.3918, 260.2110.

doi: 10.3788/COL201311.051602.

Electromagnetically induced transparency (EIT) results from a quantum destructive interference between two pathways, which is induced by another field that can render an absorptive medium transparent to the probe field[1]. It has a broad application foreground, such as the transfer of quantum correlations[2], nonlinear optical processes[3], and ultraslow light propagation[4]. Owing to the desirable properties of the EIT, EIT-like effects in plasmonics and metamaterials have been demonstrated theoretically and experimentally in recent years. These metamaterials include antennas[5], fish scale metallic patterns[6], trapped-mode patterns[7], arrays of metal rods[8], split-ring resonators (SRRs)[9], a combination of the arrays of metal rods and SRRs[10], nanoscale plasmonic resonator antennas[11], nanoscale plasmonic resonator systems[12], a hybrid plasmonic–dielectric system[13], composites of metamaterials and atomic media[14], metal nanoparticle quantum dots, and metal nanowires[15]. These EIT analogs provide an opportunity to control light propagation in nanoscales.

Considered an important technique in light propagation control, reduction of the speed of light by plasmonic and metamaterial-based EIT has drawn immense research interest. Strong capabilities in slowing down light indicate high group indexes for materials. However, the obtained group indexes that use plasmonics and metamaterials are mostly lower than 600. Despite Tang *et al.*[13] reported a group index of 2594, group indexes are generally low.

In this letter, we propose an asymmetric metamaterial that consists of two regularly spaced parallel arrays of U-shaped rings with a 90° rotation embedded in a medium. Simulations show that the metamaterial has a double EIT-like function[13] in the middle-infrared region. At low-frequency EIT-like positions, the maximum group index is 2246, whereas at high-frequency EIT-like positions, the index reaches 7474. This number is approximately thrice the maximum value reported to date. The transmittance at two transparency positions also possesses markedly high Q factors.

Figure 1(a) shows one unit cell of the metamaterial consisting of two-layered arrays of U-shaped rings embedded in a silicon medium, in which the lower layer is rotated by 90° relative to the upper one. The medium is surrounded by air. The detailed dimensions of the unit cell and one of the U-shaped rings in the cell are described in the figure caption. A light wave that is incident perpendicularly to the structure is assumed,

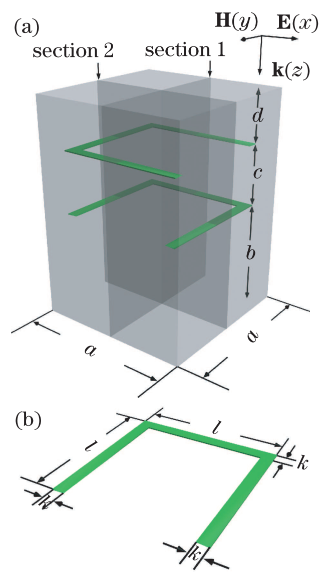

Fig. 1. (a) Schematic of one unit cell of the asymmetric metamaterial consisting of two regularly spaced parallel arrays of U-shaped rings, with the two-layered arrays embedded in a silicon medium. The geometric dimensions are as follows: $a = 1\,500$ nm, $b = 1\,015$ nm, $c = 600$ nm, and $d = 465$ nm, respectively; (b) schematic of one of the U-shaped rings in the unit cell, with geometric dimensions of $l = 1\,200$ nm and $k = 100$ nm. The thickness of each U-shaped ring is $h = 10$ nm. The thickness of the silicon medium is $D = b + c + d + 2h$. Sections 1 and 2 denote two central sections in the yz and xz planes, respectively.

with **E** polarization and **H** polarization in the x and y directions, respectively. In the following simulations, only one unit cell was considered because of the periodicity of the structure. The two-paired surfaces of the unit cell in the two periodic arrangement directions (namely, the x and y directions) are set to periodic boundary conditions. The material of the U-shaped rings in the unit cell is supposed to be a perfect conductor, which is the same as that used in Ref. [16]. As described in this reference, this assumption is acceptable for most metals in the middle-infrared region. The permittivity of the silicon medium is 11.7, as described in Ref. [17].

On the basis of the above structure, simulated transmittance as a function of frequency is shown in Fig. 2. Three resonance peaks are located at 31.56, 33.62, and 39.04 THz, respectively. The three peak values are 0.96 with a Q factor of 3156 (Q factor refers to the ratio of the center frequency to the full-width at half-maximum (FWHM) of a resonance[18]), 0.25 with a Q factor of 20, and 0.97 with a Q factor of 630. All transmittance and Q factors obtain high values at the first and third resonance peaks; this finding is similar to the EIT. The mechanism at the three resonance positions are discussed in subsequent sections. Three rings with 90° successive rotations are also discussed. Simulation results show that three resonance frequencies also exist; however, the transmittance and Q factors at these resonance positions are extremely low.

To investigate the property at the EIT-like positions, we calculated the dispersions of the transmission phase, as shown in Fig. 3(a). Strong dispersions evidently occur at the first and third resonances. The group index n_g can be calculated according to

$$n_{\mathrm{g}} = \frac{c}{v_{\mathrm{g}}} = \frac{c}{D}\tau_{\mathrm{g}} = -\frac{c}{D}\frac{\mathrm{d}\phi(\omega)}{\mathrm{d}\omega}, \quad (1)$$

where c is the speed of light in vacuum, v_g is the group velocity in the media, τ_g is the delay time, $\varphi(\omega)$ is the phase as a function of the angular frequency ω, and D is the spacing in the z direction. The group index n_g as a function of frequency is plotted in Fig. 3(b). All group indexes at the two resonances are extremely high at 2246 and 7474, respectively. These large values indicate that such a metamaterial can efficiently reduce the speed of light.

We then investigated the influence of U-shaped ring numbers in the unit cell on transmittance and resonance positions. We simulated transmittances for two additional cases: 1) where the lower ring is removed, and 2) where the upper ring is removed. The corresponding

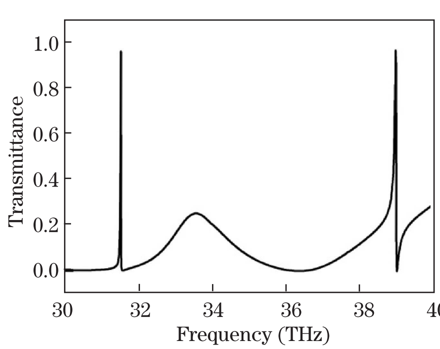

Fig. 2. Transmittance as a function of frequency.

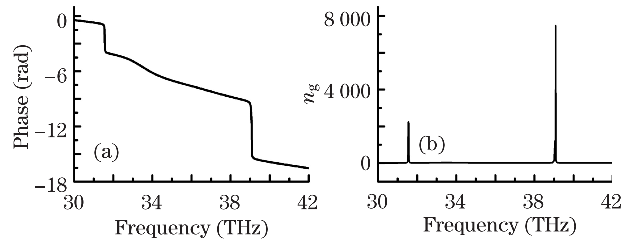

Fig. 3. (a) Transmission phase and (b) group index as a function of frequency.

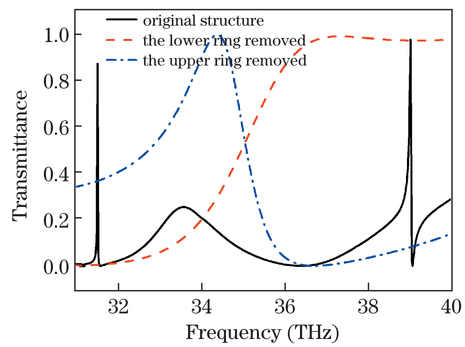

Fig. 4. (Colur online) Transmittance as a function of frequency for three cases. The solid black curve (i.e., the curve in Fig. 2) represents the original structure. The dashed red curve shows the case when the lower ring is removed. The dash-dot blue curve shows the case when the upper ring is removed. The other parameters are the same as those in Fig. 2.

results are shown in Fig. 4, where the curve in Fig. 2 is also plotted. No obvious resonance peak is observed in the structure where the lower ring is removed. Only one resonance peak occurs, and the transmittance with high Q factors disappears when the upper ring is removed. Evidently, the ring numbers and its position dramatically affect resonance.

To investigate the physical mechanism for the production of high-Q factor transmittance in Fig. 2, the current distributions (as plotted directly using the HFSS software) in the U-shaped rings at the three resonances are discussed, as shown in Figs. 5(a)–5(c). Figure 5(a) shows that almost no current flows in the upper U-shaped ring at the first resonance. As indicated, the upper ring does not participate in resonance, whereas the lower ring does. By contrast, current flows in the upper U-shaped ring at the third resonance (see Fig. 5(c)), suggesting that the upper ring participates in resonance. However, at the second resonance, current is distributed in the upper and lower rings (see Fig. 5(b)); thus, the two rings simultaneously contribute to resonance. The findings also suggest that each U-shaped ring consists of three sections of wires. Every wire can be considered as an electric dipole. Meanwhile, the arrows indicate the directions of the dipoles. Hence, any current distribution can be interpreted to consist of different electric dipoles[19] excited by the incident electromagnetic field.

To illustrate, Fig. 5(a) shows two parallel and inphase dipoles radiating in different directions, including the forward direction. When the radiated electromagnetic waves encounter the lower surface, a part of the waves

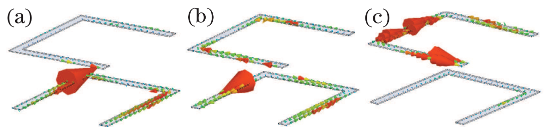

Fig. 5. (Color online) Current distributions in the two rings at resonance frequencies of (a) 31.56 (the first resonance), (b) 33.62 (the second resonance), and (c) 39.04 THz (the third resonance) in Fig. 2, respectively.

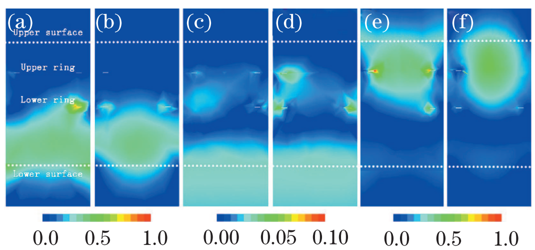

Fig. 6. (Color online) Electric field distributions in different cross-sections at different resonance frequencies in the unit cell. Electric field distributions at (a) section 1 and (b) section 2 corresponding to Fig. 1 at 31.56 THz; electric field distributions at (c) section 1 and (d) section 2 corresponding to Fig. 1 at 33.62 THz; electric field distributions at (e) section 1 and (f) section 2 corresponding to Fig. 1 at 39.04 THz.

is reflected. A mode field that satisfies the constructive interference condition is formed between the lower ring and the lower surface, as shown in Figs. 6(a) and 6(b). Enhanced transmittance with a high Q factor thus occurs, which causes the first transmittance peak in Fig. 2.

Contrary to the case in Fig. 5(a), three dipoles are shown in Fig 5(c). Two of these three dipoles move in opposite directions. The radiation is thus restrained, forming a dark mode in the ring (see Figs. 6(e) and 6(f)) Meanwhile, a radiative mode is also observed. The coupling between the radiative mode and the dark mode induces transparency with a high Q factor. This physical mechanism is similar to that proposed by Zhang *et al.*[20].

For the case presented in Fig. 5(b), the dipoles formed in the two rings produce a radiative mode rather than a dark mode, as shown in Figs. 6(c) and (d). Thus, the second resonance in Fig. 2 possesses an extremely low Q factor.

In conclusion, we propose an asymmetric metamaterial based on two regularly spaced parallel arrays of U-shaped rings. The simulation results demonstrate that the structure exhibits a double EIT-like phenomenon and enhanced transmission with extremely high group indexes and Q factors. Notably, at the high-frequency EIT-like position, the group index reaches thrice the maximum value reported to date. Additionally, the transparency originates from the mode field. This finding satisfies the constructive interference condition at the lower-frequency resonance, as well as the coupling between the radiative mode and the dark mode at the higher-frequency resonance, respectively. Such a metamaterial can be used as a subwavelength-scale light controller, which has potential applications in optoelectronics. Another advantage is the ease of integration with other devices compared with traditional methods because of its small size.

This work was supported by the National Natural Science Foundation of China (No. BK2011203), the Graduate Innovation Project of Jiangsu Province (No. CXLX110908), and the Priority Academic Program Development (PAPD) of Jiangsu Higher Education Institutions, China.

References

1. K. J. Boller, A. Imamolu, and S. E. Harris, Phys. Rev. Lett. **66,** 2593 (1991).
2. Y. Zhang, K. Hayasaka, and K. Kasai, Phys. Rev. A **71,** 062341 (2005).
3. S. Harris and L. Hau, Phys. Rev. Lett. **82,** 4611 (1999)
4. H. Gersen, T. J. Karle, R. J. Engelen, W. Bogaerts, J. P. Korterik, N. F. van Hulst, T. F. Krauss, and L. Kuipers, Phys. Rev. Lett. **94,** 073903 (2005).
5. S. Jarchi, J. R. Mohassel, and R. F. Dana, J. Electromagn. Waves Appl. **24,** 755 (2010).
6. G. Dolling, C. Enkrich, M. Wegener, C. M. Soukoulis, and S. Linden, Science **312,** 892 (2006).
7. V. A. Fedotov, M. Rose, S. L. Prosvirnin, N. Papasimakis, and N. I. Zheludev, Phys. Rev. Lett. **99,** 147401 (2007).
8. Z. G. Dong, H. Liu, J. X. Cao, T. Li, S. M. Wang, S. N. Zhu, and X. Zhang, Appl. Phys. Lett. **97,** 114101 (2010).
9. Z. G. Dong, S. Y. Lei, M. X. Xu, H. Liu, T. Li, F. M. Wang, and S. N. Zhu, Phys. Rev. E **77,** 056609 (2008).
10. M. Kang, H. X. Cui, Y. Li, B. Gu, J. Chen, and H. T. Wang, J. Appl. Phys. **109,** 014901 (2011).
11. R. Kekatpure, E. Barnard, W. Cai, and M. Brongersma, Phys. Rev. Lett. **104,** 243902 (2010).
12. H. Lu, X. Liu, D. Mao, Y. Gong, and G. Wang, Opt. Lett. **36,** 3233 (2011).
13. B. Tang, L. Dai, and C. Jiang Opt. Express **19,** 628 (2011).
14. P. Weis, J. L. Garcia-Pomar, R. Beigang, and M. Rahm, Opt. Express **19,** 23573 (2011).
15. M. T. Cheng and Y. Y. Song, Opt. Lett. **37,** 978 (2012).
16. N. I. Zheludev, S. L. Prosvirnin, N. Papasimakis, and V. A. Fedotov, Nat. Photon. **2,** 351 (2008).
17. E. D. Palik, *Handbook of Optical Constants of Solids* (Academic Press, New York, 1985).
18. I. A. I. Al-Naib, C. Jansen, N. Born, and M. Koch, Appl. Phys. Lett. **98,** 091107 (2011).
19. C. J. F. Böttcher, P. Bordewijk, and O. C. Belle, *Theory of Electric Polarization* (Elsevier, Amsterdam, 1973).
20. S. Zhang, D. A. Genov, Y. Wang, M. Liu, and X. Zhang, Phys. Rev. Lett. **101,** 047401 (2008).